(2)

PROCESSING, FABRICATION, AND DEMONSTRATION OF HTS INTEGRATED MICROWAVE CIRCUITS

APPENDIX A
Papers Accepted for Publication

1. A. Davidson, J. Talvacchio, M. G. Forrester, and J. R. Gavaler, "Superconductive Electronics with High Transition Temperature Films," Proc. ICMC, Advances in Cryogenic Engineering (Materials), Vol. 39, (Plenum, New York, 1993).
2. B. Han, D. A. Neumeyer, B. H. Goodreau, and T. J. Marks, "In-Situ MOCVD of Dielectric Materials for High-T_c Superconducting Devices," Proc. ICMC, Advances in Cryogenic Engineering (Materials), Vol. 39, (Plenum, New York, 1993).
3. B. H. Goodreau, B. J. Hinds, and T. J. Marks, "Synthesis and Metal Organic Vapor Deposition of ^{t}Butyl Substituted Cyclopentadienyls of Barium," Chemistry of Materials, 1993.

Superconductive Electronics with High Transition Temperature Films

A. Davidson, J. Talvacchio, M.G. Forrester, and J.R. Gavaler

Westinghouse Science and Technology Center
1310 Beulah Road
Pittsburgh, PA 15235

ABSTRACT

Electronics based on high transition temperature superconductive thin film materials is presently viable in some important niches, particularly in passive microwave circuits. Applications requiring Josephson junctions are impeded by the lack of reproducible junctions, but the junctions that can be produced are good candidates for the new Rapid Single Flux Quantum class of extremely fast digital circuits. Other devices that take advantage of the weak fluxoid pinning of some films are also promising, particularly the flux flow transistor. The availability of both Josephson and flux flow devices at 77K invites exploration of hybrid technologies using HTS multi-chip modules supporting silicon CMOS chips and superconductive chips at the same time. The superconductive contribution to the emerging applications can result in significant performance advantages, particularly in remote sensing and communications.

INTRODUCTION

The Rapid Single Flux Quantum[1] (RSFQ) Josephson junction family of digital circuits was invented before the discovery of high temperature superconductivity. The flux flow transistor[2] (FFT) was developed using classic helium temperature superconductive materials. Superconductive microwave devices[3] are also not new. CMOS semiconductors have been developed for reasons having nothing at all to do with competition from superconductive devices. But all of these independent advances are now linking up with one another as a result of the discovery and unique material properties of high temperature superconductivity (HTS) oxides, and the steady improvement of HTS thin films and structures. Applications in radar and communication using passive devices[4] are most imminent, because the structures are simple, and the improvement over the normal-state equivalent is large. Signal processing and data switching circuits are also under development, but will require a lot more materials understanding to be equally advantageous. This paper reviews the progress that has been made in depositing high

quality HTS films on appropriate substrates, and relates this progress to device and circuit properties needed for various applications.

FILMS

Many other papers in this conference deal with the details and complexities of film deposition. Here we list two of the major techniques used now, with some comments on the relative merits. Despite a lot of early work using coevaporation[5], the presently preferred methods are sputtering[6] and laser ablation[7]. These work in similar ways. They both involve transport of material from a stoichiometric target to a heated substrate. In ablation this transport is accomplished by focusing a nanosecond scale laser pulse of sufficient energy onto the target. The pulse heats the target immediately under the surface, vaporizing it, and causing an explosive discharge of material perpendicular to the target surface. Some of the ejected material is energetic enough to be in the form of a plasma; some is apparently in the form of particles and droplets. A heated substrate a few centimeters away collects the material to build up a film. Laser ablated films are typically of high quality, with excellent stoichiometry, and good supercondcutive parameters.Work is progressing to improve surface roughness, and to handle larger (>5 cm) wafers. The deposition rate for small wafers, however is fairly rapid, typically a few Angstroms per second.

The sputtering method is in many ways complementary to laser ablation. It is slow, often in the range of 0.1 Angstroms per second. It is easy to scale up to large wafers, with 5 cm diameters common, and 10 cm under development. The most common kind of sputtering is with rf magnetron systems, using an off-axis geometry. In the off-axis arrangement, the substrates are orthogonal to the target, and usually off to the side, to avoid direct bombardment by negative ions. These are ionized oxygen atoms, which can come from either the sputter gas or the target itself, and which are energetically emitted from the target. Under conditions which minimize resputtering from hot surfaces in the vicinity of the substrate, sputtered YBCO films were the first to be grown without the presence of CuO precipitates. Smooth films resulting from the elimination of CuO particles have also been produced by laser ablation by employing an off-axis configuration[8]. The off-axis configuration reduces the high-deposition-rate advantage of laser ablation compared to sputtering. The ultimate importance of uniform deposition on large wafers should be emphasized. For this purpose other deposition techniques such as MOCVD[9] may prove to be the best technique. For now, however, ablation and sputtering produce the best films.

Choice of substrate is extremely important to the successful completion of useful circuits. $SrTiO_3$ substrate[10] can be used to grow very high quality films, but with an extraordinarily high dielectric constant, which rules it out for any high speed applications. $LaAlO_3$[11] has a much lower dielectric constant, approximately 24, and has been used successfully for single layer applications, such as microstrip or co-planar microwave filters and delay lines. It has not worked so well for multi-layer circuits, however, because of motion of twin boundaries[12] when the wafer is heated for application of new HTS layers. The moving twins can shift the bottom film layers by several microns over the width of even a one centimeter chip, making alignment of subsequent layers impossible. At the moment, $NdGaO_3$[13] appears to be the substrate of choice for multilayer circuits. It has a low dielectric constant, similar to $LaAlO_3$, but without the shifting twins.

Consideration of multi-layer structures also determines the choice of HTS film material. The materials with the highest T_c's are TBCCO,and, recently, HgBCCO[14], but their lack of stability means that for now there is no way to produce multiple levels. YBCO has proven to have the best combination of transition temperature and superconductive properties, and with enough stability so that subsequent layers can be formed without degradation of prior layers.

In addition to superconducting films, epitaxial insulating films are required in multilayer superconducting circuits for isolation of ground planes, crossovers, lumped-element capacitors and inductors, and flux transformers. Epitaxial growth is not necessarily required to obtain desired properties for the insulator but is necessary to support growth of subsequent high-quality superconducting film layers. The obvious candidate materials for epitaxial insulators are the same ones that work well as substrates. Other oxide and fluoride compounds which, for example, cannot oe grown as large single crystals, but have a good lattice match to YBCO have been tested. Figure 1 summarizes the dielectric loss properties of various thin-film dielectrics studied at Westinghouse in comparison with minimum requirements estimated for several applications. The loss tangent is based on data from bulk samples and the dc resistivity at 77K was measured on parallel-plate capacitor structures with YBCO on the bottom or on both sides. Both the $SrTiO_3$ and Sr_2AlTaO_6 (SAT)[15] grew as pinhole-free films but SAT is the better choice for most applications based on lower values of both the real and imaginary parts of its dielectric constant.

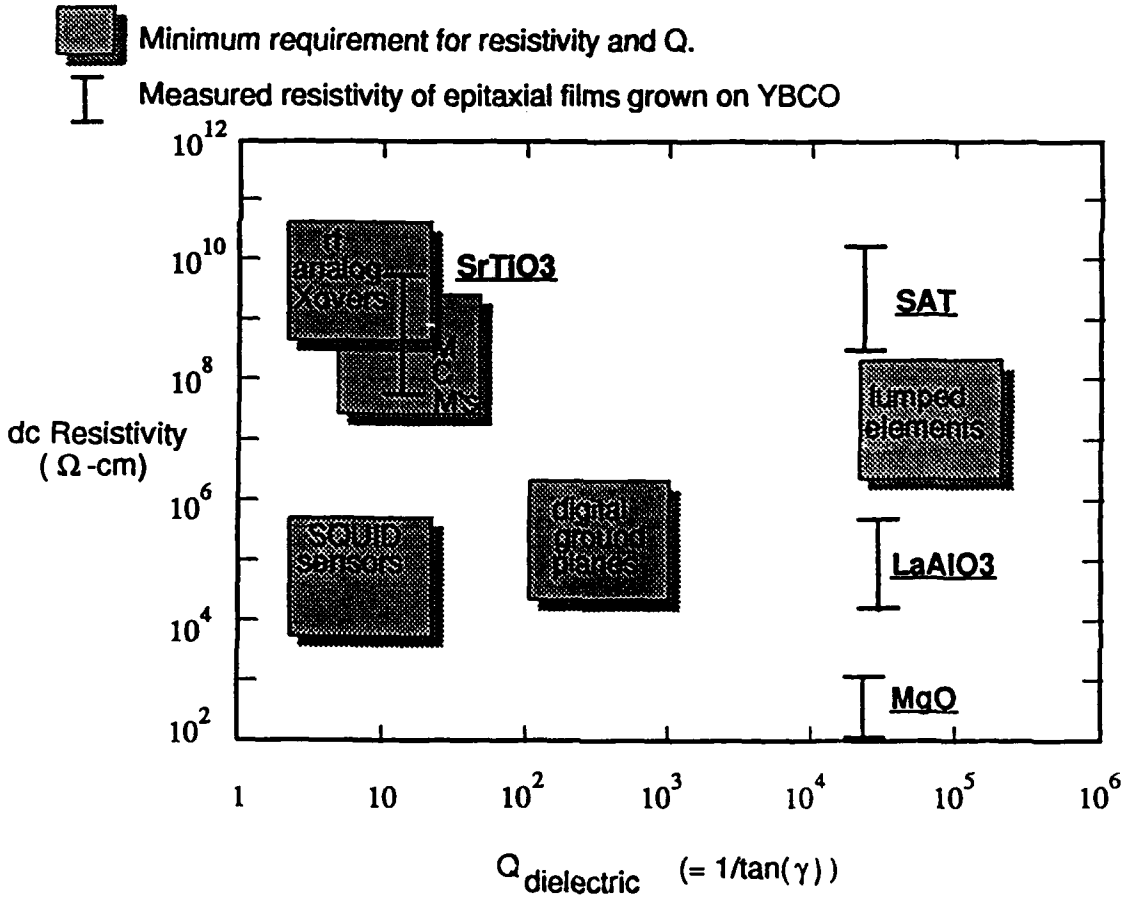

Fig. 1. Requirements for HTS dielectrics, and the performance of some known examples. These films grow epitaxially on appropriate substrates, and support epitaxial growth of YBCO.

It is possible to find substrate materials that are compatible with both HTS films and ordinary semiconductor devices, so that hybrid circuits for usc in liquid nitrogen can be produced monolithically[16]. For example, a layer of silicon can be grown epitaxially on

sapphire, and formed into semiconductor circuits. This technology has a long history and is known as Silicon on Sapphire, or SOS. After the transistors are formed, areas for the HTS devices can be stripped down to the substrate, and with appropriate buffer films, good YBCO layers can be grown as well. The 750 C temperature will not hurt the transistors, particularly if the HTS deposition is quick, as in laser ablation.

HTS Applications

We can expect commercial and military use of HTS films for microwave passive components, such as filters or delay lines, in the near future; and as ground planes and interconnection wires on multi-chip modules further out in time. Passive microwave devices using HTS films are particularly attractive because they combine very low insertion loss with small size and low weight. In fact, even including the necessary refrigeration, use of such devices still saves space and weight, and provides a performance edge[17]. A prototype Westinghouse X-band filter is shown in Fig. 1, and the measured performance of a prototype bank of four filters[18] is shown in Fig. 2.

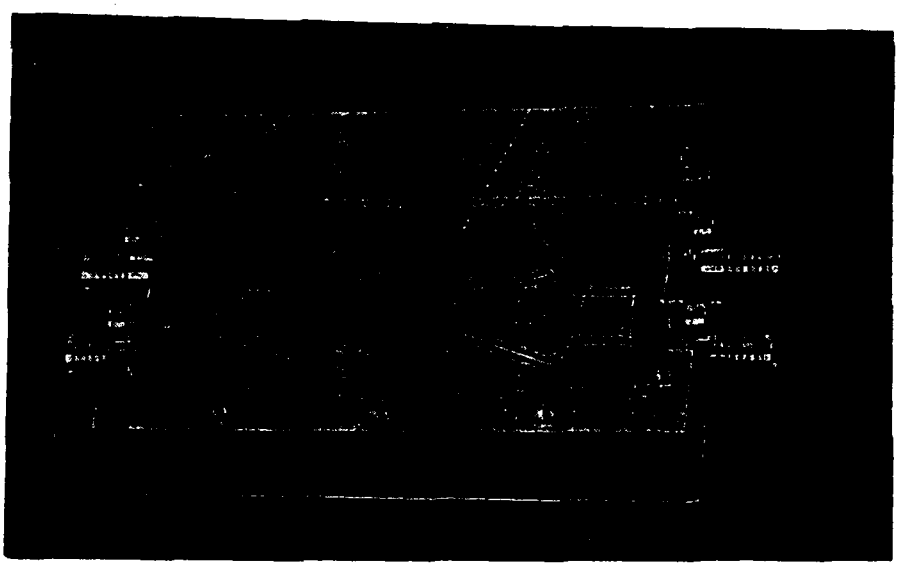

Fig. 2. A Westinghouse 4 GHz HTS filter. The wafer is approximately 5 cm long. Such filters will outperform normal components with dimensions of 30 or more cm, and weighing many kilograms.

In the longer term, HTS film structures can be expected to play a key role in the interconnection of semiconductor chips[19]. CMOS silicon devices work better at 77K than at room temperature. The operating voltage is lower, there is less dissipation, and switching is faster. By putting low temperature silicon chips on a HTS board, this speed advantage

can be increased because of the nearly lossless characteristics of HTS microstrip transmission lines. The advantage could be increased even further if hybrid CMOS HTS circuits are developed to drive these transmission lines.

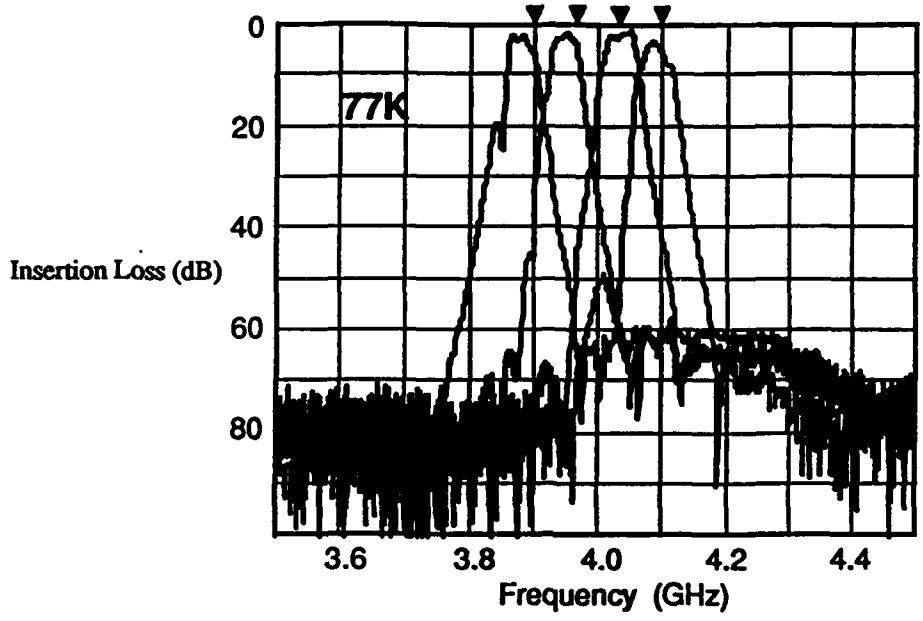

Fig. 3. Measured characteristics of the Westinghouse prototype filter bank. The four triangles at the top mark the intended center frequencies.

HTS Active Devices

The classical superconductive active device is the Josephson junction, in one form or another. Several other types of active devices have also been developed in classical technology, including FET-like and bipolar-like devices[20], and also a rather successful group of devices which control the movement of magnetic flux, or flux-flow devices. In HTS technology at present, two types have achieved some success, the Josephson junction and the flux flow devices. However, the relative success of these two are reversed, relative to classical superconductive technology. The flux flow devices in many ways take advantage of some natural properties of HTS material, whereas Josephson junctions have to fight against them.

Josephson junctions

It is very difficult to make the exact analog of a classical Josephson junction out of HTS materials. The trouble stems from a combination of extreme anisotropy due to the layered nature of HTS superconductors, and their very short coherence lengths (roughly 3 to 30 Angstroms). This means that superconductivity, and hence the Josephson effects, are suppressed at almost all interfaces of these materials. Usable junctions, however, have been made in some clever ways.

For electronics the most successful methods so far involve "edge junctions[21]," where some property or configuration is altered where a film goes up over an edge of an underlying film, usually an insulator. In some cases, a thin normal metal at the edge provides the coupling between films, in others a deposited oxide is used. Fig. 4 shows a typical step-edge geometry where gold couples to HTS films across a small (100 nm) gap.

The edge geometry does produce the distinctive features of a classical non-hysteretic Josephson junction. Where parasitic capacitance has been large, hysteresis has also been observed but never with a true gap structure. Therefore these junctions are not suited for many of the classical superconductive circuit families that require hysteresis or a sharp gap.

There is one class of digital circuits which require just what HTS edge Josephson junctions seem to deliver, and that is the Rapid Single Flux Quantum[1,22] (RSFQ) type of circuit. RSFQ circuits do not use voltage or current levels to represent ones and zeroes, as all transistor and most superconducticive circuits do. Rather, bits are represented by the presence or absence of quantized fluxoids in different parts of the circuits.

Quantization of magnetic flux is an integral part of superconductive circuits, where the magnetic flux enclosed by a superconductive path is forced to take on a value corresponding to an integral multiple of $\Phi_0 = 2.07 \times 10^{-15}$ Webers. It is relatively simple, by controling inductance and critical current values, to control the motion of single flux quanta, or fluxons, in superconductive circuits using Josephson junctions. Fig. 5 below compares a simple RSFQ circuit for transmitting fluxons to a mechanical analog. The marble clearly corresponds to the fluxon, and the spring loaded gates are roughly analagous to Josephson

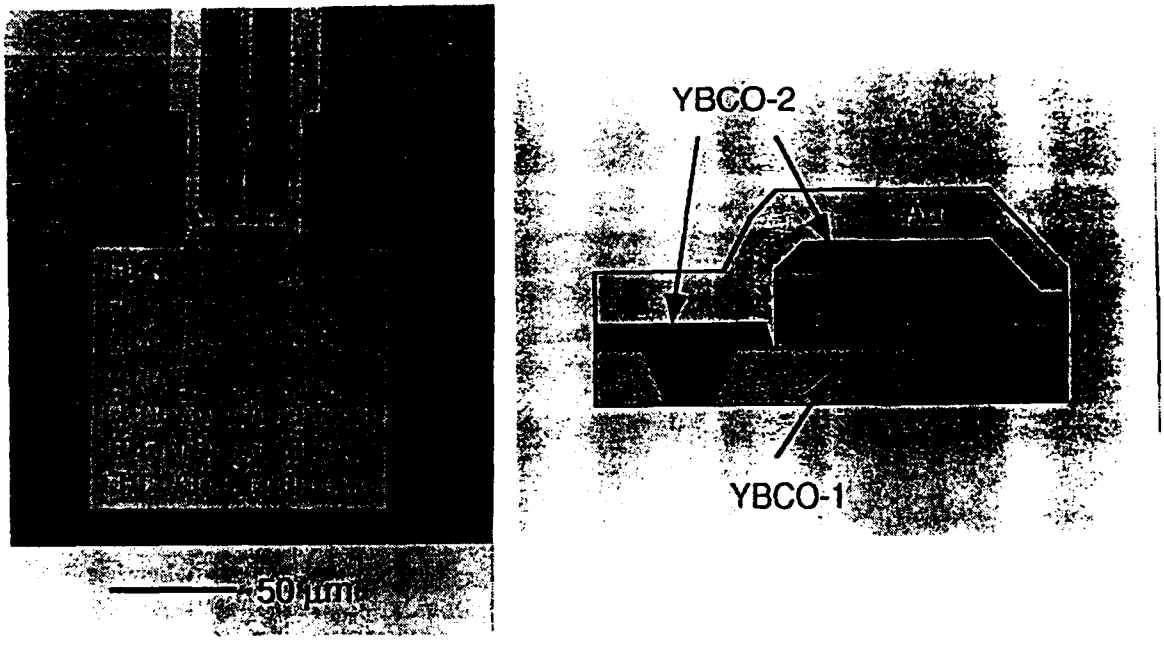

Fig. 4. Configuration of an HTS step-edge Josephson junction. On the right is a schematic cross section, showing the two layers of YBCO, the insulating step, and the gold layer that provides the Josephson coupling. On the left is a top view of a device fabricated at Westinghouse using this structure.

junctions. The bias current exerts a force on the fluxon, via the Lorentz force, as gravity applies a force to the marble. It is possible to achieve any logic function using some fluxons to control the motion of other fluxons through their interaction with the Josephson junctions. In this approach it is necessary to use some Josephson junctions to allow surplus fluxons to escape from the circuit, as one could use spring loaded gates in the mechanical analog as trap doors to dispose of excess marbles.

The focus of research on edge junctions is to find ways to minimize the spread in critical current values. At present it is common for junctions on the same chip to have a critical curent spread of 50% or more, though some have been produced with spreads of only about 20%. This magnitude of variation is sufficient for only the smallest digital

circuits, with at most a few dozen junctions. To fulfill the potential of RSFQ circuits with thousands of junctions, critical current spreads of at most a per cent or two will have to be developed. At the moment, a certain type of nanobridge junction[23] is much better than the edge geometry for minimizing current spread, but these junctions have critical currents too low for reliable operation at liquid nitrogen temperature, and are not amenable to higher currents.

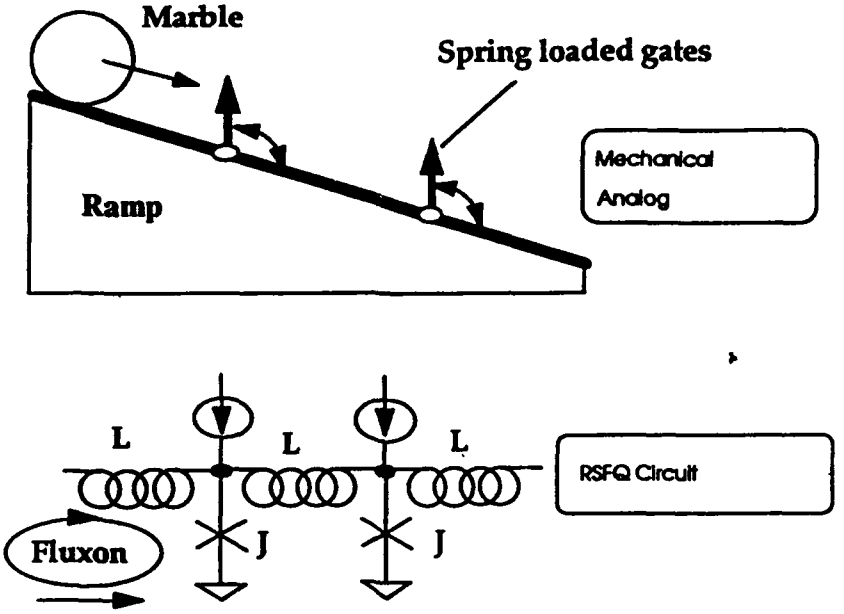

Fig. 5. Comparison of simple RSFQ circuit to a mechanical analog. The Josephson circuit treats the fluxon as conserved particle, forced through the circuit by bias currents, like the marble forced down the ramp by gravity. The Josephson junctions, labeled with J's, act like the spring loaded gates that interact with the marble on the ramp.

Flux Flow Transistors

HTS thin films, particularly those based on thallium compounds, allow fluxons to flow relatively freely through them. This property is referred to as "weak pinning," and is the basis for the Flux Flow Transistor (FFT), a true three-terminal superconductive device[24]. Figure 5 schematically compares the control of flux motion in an FFT to charge motion in an FET. Figure 6 shows the IV curve of a large scale FFT a few millimeters on a side, made from a piece of bulk ceramic YBCO, with a coil wound around it. For a load of a few milliohms, it is apparent that this device has both current and voltage gain. Smaller devices fabricated with thin films have produced similar gain or transimpedance, with much smaller currents and higher voltage.

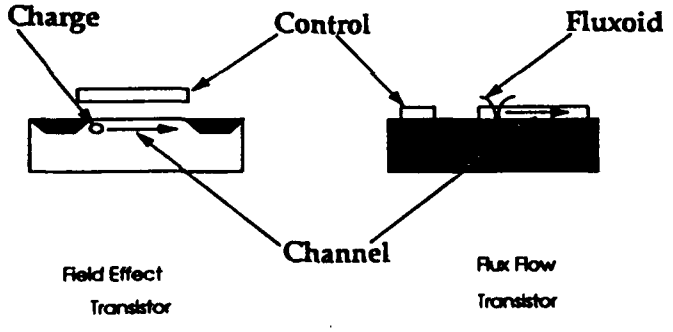

Fig. 6. Analogy between charge transport in the channel of an FET and magnetic flux transport in the channel (HTS thin film) of an FFT.

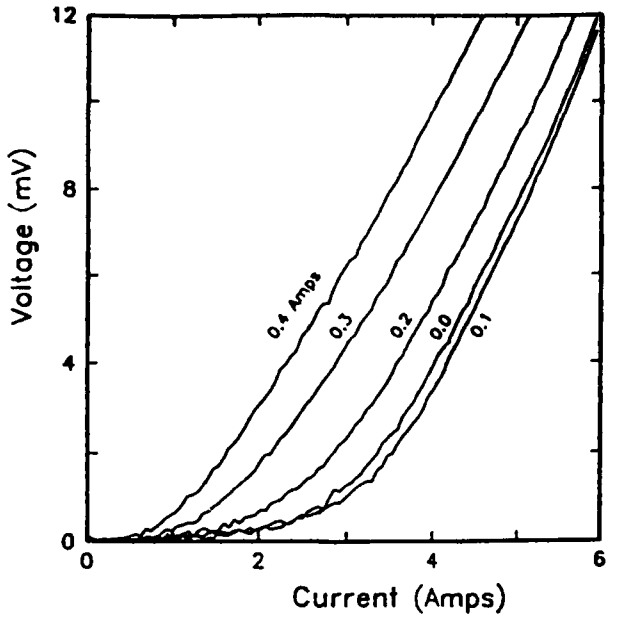

Fig. 7. Current-voltage characteristics of HTS bulk FFT device. Veteran engineers will note the similarity to vacuum triode characteristics.

Martens[24] has shown many circuits using these devices, including microwave amplifiers, oscillators, and digital logic and memory. From a circuit view point, the main problem with these devices is that they are so far pretty leaky. That is, the high resistance state is still a fairly low resistance, generally a few ohms. Strongly in their favor is that they can be made from a a single HTS film deposition, and they have been reported to have very high effective $I_c R_n$ products, sometimes over 10 millivolts. They are therefore a natural for interfacing to semiconductors.

There are opportunities to use flux flow superconductive devices as amplifiers in significant military and civilian applications. These opportunities have to do with the interconnection of fast but very low voltage Josephson junction devices with the semiconducting devices, such as CMOS circuits. This type of interconnection could take at least two forms. In the first form, the CMOS circuits are the ultimate destination of the outputs of the Josephson circuits. For example, in communications, a Josephson signal processor in a cryogenic environment is of no value unless there is a way of reading the cryogenic output bytes into conventional computing equipment.

The other type of interconnection would be between Josephson circuits and CMOS circuits all in the dewar. There is at least one proposal[25], for example, to use Josephson devices as output drivers for FET memory cells. In the processor, where the memory bytes are received, another superconductive circuit would be used to pick up the low level signal, and deliver it to another semiconductor.

Multi-Chip Modules

A natural application for HTS thin films is in multi-chip-module[19] (MCM) technology. Here the idea is to eliminate one level of packaging for chips. In present desk-top computers, for example, chips are mounted in epoxy packages with multiple pins sticking out, to be plugged into sockets or soldered directly to printed circuit boards. MCMs eliminate the epoxy package. Bare chips are mounted to the board by various techniques, including wire bonding, and flip-chip soldering. If the printed circuit board

were constructed of HTS thin films and appropriate dielectrics, several advantages could accrue. Because resistance is eliminated, the wiring channels could be put on a much finer pitch, which could greatly simplify the construction of the boards. Power and ground planes would be more ideal, helping to eliminate cross talk and power dips. It should be possible to build high quality transmission line structures, with either strip line or coplanar geometries. If terminations can be used, these lines could be charged up by one-way transmission of the signal, and so HTS MCMs could also be significantly faster than normal metal boards, which rely on multiple reflections to transfer data. The challenge here is to find ways to grow high quality HTS films in multiple layers with compatible insulators, and to do this with materials having an acceptable thermal expansion match to the chips and connectors. Also needed are stable and reliable interface materials for all the connections, and some means of modification and repair.

ACKNOWLEDGEMENTS

We wish to express our gratitude for data, and helpful consultation to Salvador Talisa, John X. Przybysz, Mike Janocko, Don Miller, Dan Meier, Joon-Hee Kang, Hodge Worsham, and George Wagner. This work was supported in part by ONR/ARPA Contract No. N00014-91-C-0112, AFOSR Contract No. F49620-91-C-0034, and NRL Contract No. N00014-92-C-2043.

REFERENCES

1. K.K. Likharev, O.A. Mukhanov, and V.K. Semenov, "Resistive Single Flux Quantum Logic for Josephson Junction Technology," in SQUID'85, Berlin, Germany: W. de Gruyter, 1985, pp.1103-1108.
2. D.P. McGinnis, J.E. Nordman, and J.B. Beyer, "Optimization of Circuit Parameters for the Vortex Flow Transistor," IEEE Trans. Mag., MAG-23, 699 (1987).
3. R.A. Davidheiser, "Superconducting Microstrip Filters," AIP Conference Proceedings No. 14, Future Trends in Superconducting Electronics, Edited by B.S. Deaver, C.M. Falco, J.H. Harris, and S.A. Wolf, AIP, New York, 1978, pp. 219-222.
4. M. Nisenoff, J.C. Ritter, G. Price, and S.A. Wolf, "The High Temperature Superconductivity Space Experiment," IEEE Trans. Appl. Supercond. Vol. 3, 2885 (1993).
5. J. M. Phillips, M. P. Siegal, C. L. Perry, and J. H. Marshall," Comparison of Ba2YCu3O7-d Films on NdGaO3 and LaAlO3," IEEE Trans. Magn. 27 (2), 1006 (1991).
6. J. R. Gavaler, J. Talvacchio, T. T. Braggins, M. G. Forrester, and J. Greggi, "Critical Parameters in the Single-Target Sputtering of YBa2Cu3O7," J. Appl. Phys. 70(8), 4383 (1991).
7. T. Venkatesan, X. Wu, A. Inam C. C. Chang, M. S. Hegde, and B. Dutta, "Laser Processing of High-Tc Superconducting Thin Films," IEEE J. Quantum Elec. 25(11), 2388 (1989).
8. Robin J. Kennedy, " A New Geometry for Laser Ablation for the Production of Smooth single Layer YBCO/PBCO Multilayer Films," Adv. in Cryo. Eng. (Materials) Vol. 138, 1005. Edited by F.R. Fickett and R.P. Reed, Plenum Press, New York, 1992.
9. A. Erbil, K. Zhang, B. S. Kwak, and E. P. Boyd, "Review of Metalorganic

Chemical Vapor Deposition of High-Temperature Superconducting ThinFilms," in Processing of Films for HTS Electronics, edited by T. Venkatesan (SPIE 1187, Bellingham, WA, 1990) pp. 104.

10. P. Chaudhari, R. H. Koch, R. B. Laibowitz, T. R. McGuire, and R. J. Gambino, Critical Current Measurements in Epitaxial Films of $YBa_2Cu_3O_{7-x}$," Phys. Rev. Lett. 58, 2684 (1987).
11. R.W. Simon, "Substrates for HTS Films," in Processing of Films for HTS Electronics, edited by T. Venkatesan (SPIE1187, Bellingham, WA, 1990) pp. 2.
12. Gong-Da-Yao, Shang-Yun Hou, M. Dudley, and J.M. Phillips, " Synchrotron X-Ray Topography Studies of Twin Structures in Lanthanum Aluminate Single Crystals," J. Mater. Res. 7, 1847 (1992).
13. M. Sasaura, S. Miyazawa, and M. Mukaida, "Thermal Expansion Coefficients of High-Tc Superconductor Substrate $NdGaO_3$ Single Crystal," J. Appl. Phys. 68(7), 3643 (1990).
14. A. Schilling, M. Cantoni, J.D. Guo, and H.R. Ott, "Superconductivity above 130K in the Hg-Ba-Cu-O System," Nature 30, 56 (1993).
15. A.T. Findikoglu, C. doughty, S. Bhattacharya, Qi Li, X.X. Xi, T. Venkatesan, R.E. Fahey, A.J. Strauss, and Julia M. Phillips, "Sr2AlTaO6 Films for Multilayer High-Temperature Superconducting Device Applications," Appl. Phys. Lett. 61, 1718 (1993).
16. M.J. Burns, P.R. de la Houssaye, S.D. Russell, G.A. Garcia, S.R. Clayton, W.S. Ruby, and L.P. Lee, "Demonstration of YBCO and Complementary Metal Oxide Semiconductor Device Fabrication on the same Sapphire Substrate," to be published, Appl. Phys. Lett. 63 (1993).
17. Invited presentations at the "High Tc Superconductivity in Microwave Systems: A Technology Assessment," Workshop, 1993 International Microwave Symposium, Atlanta, GA, June, 1993. R.R. Bonetti, M. Nisenoff, NRL, COMSAT Laboratories, D.L. Johnson, JPL.
18. Data kindly provided prior to publication by S. Talisa and M. Janocko, Westinghouse STC, Pittsburgh, PA 15235.
19. M.J. Burns, K. char, B.F. Cole, W.S. Ruby and S.A. Sachtjenh, "Multichip Module using Multilayer $YBa_2Cu_3O_7$ Interconnects, Appl. Phys. Lett., 62, 1435 (1993).
20. D.J. Frank and A. Davidson, "Prospects for High-Tc supercondcutor/Semiconductor transistor like devices", 5th International Workshop on Future Electron Devices, Miyagi, Japan, June 1988
21. R.P. Robertazzi, R.H. Koch, R.B. Laibowitz, and W.J. Gallagher, "$Y_1Ba_2Cu_3O_7/MgO/Y_1Ba_2Cu_3O_7$ " Appl. Phys. Lett. 61, 711 (1992).
22. K.K. Likharev and V.K. Semenov, "RSFQ Logic/Memory Family," IEEE Trans. Appl. Supercond. 1, 3 (1991).
23. J.R. Wenot, J.S. Martens, C.I.H. Ashby, T.A. Plut, V.M. Hietala, Cc.P. Tigges, D.S. Ginley, M.P. Siegal, J,M, Phillips and G.K.G. Hohenwarter, "YBCO Nanobridges Fabricated by Direct-Write Electron Beam Lithography," Appl. Phys. Lett. 61, 1597 (1992).
24. J. S. Martens, V.M. Hietala, T.A. Plut, D.S. Ginley, G.A. Vawter, C.P. Tigges, M.P. Siegal, Julia M. Phillips, and S.Y. Hou, "Flux Flow Microelectronics," IEEE Trans. Appl. Supercond., vol. 3, 2295 (1993).
25. Harry Kroger and Uttam Ghoshal, "Can Superconductive digital Systems Compete with Semiconductor Systems?" IEEE Trans. Supercond., Vol. 3, 2307 (1993).

IN SITU MOCVD OF DIELECTRIC MATERIALS FOR HIGH-T_c SUPERCONDUCTING DEVICES

Bin Han, Deborah A. Neumayer, Bruce H. Goodreau and T. J. Marks*

Department of Chemistry, the Materials Research Center, and
the Science and Technology Center for Superconductivity
Northwestern University, Evanston, IL U.S.A. 60208-3113

INTRODUCTION

The development of new, chemically compatible, lattice and thermal expansion-matched, low dielectric constant, and low dielectric loss materials for use as insulators, dielectrics, buffers, and overlayers represents a critical need for the development of high temperature superconductor (HTS)-based electronics.[1-6] Although epitaxial growth of high-T_c thin films is well developed, the fabrication of passive and active microelectronic devices with HTS materials depends not only on the deposition of epitaxial HTS thin films but also on the successful growth of epitaxial dielectric thin films. We overview here *in situ* growth studies of $NdGaO_3$, $YAlO_3$, $PrGaO_3$, and Sr_2AlTaO_6 (SAT) thin films as the first step in superconductor-insulator-superconductor (S-I-S) structure fabrication by metal-organic chemical vapor deposition (MOCVD). As in the case of HTS film growth,[7-10] MOCVD offers the attraction of simplified apparatus, low growth temperatures, and suitability for large scale/area depositions on substrates having complex shapes. For MOCVD derived perovskite dielectric films,[11] compatibility with various HTS deposition processes represents a crucial test of the utility of this growth technique. Among the potential substrate materials for epitaxial deposition of HTS films,[1,6,12,13] the perovskite materials $NdGaO_3$, $YAlO_3$, $PrGaO_3$, and Sr_2AlTaO_6 have small lattice-mismatches with HTS materials, are chemically compatible with HTS materials, are thermally stable, and have good dielectric properties. The physical and electrical properties of the dielectric perovskites thus make them well suited for HTS electronics applications. In the present work, the microstructure, surface morphology, and film-substrate interface of MOCVD-derived perovskite films have been characterized by X-ray diffraction (XRD), scanning electron microscopy (SEM), energy-dispersive X-ray analysis (EDX), cross-sectional high resolution electron microscopy (HREM), and selected area diffraction transmission electron microscopy (TEM).

---

* Author to whom correspondence should be addressed

STRATEGIES FOR PRECURSOR DESIGN, DEPOSITION METHODOLOGY AND FILM CHARACTERIZATION

Precursor Design

A requisite property for all MOCVD precursors is suitable volatility. An attractive strategy to achieve this volatility is to minimize lattice cohesive energies by encapsulating the metal ion in a sterically saturating nonpolar ligand environment. For large trivalent ions (especially Y^{+3}, Pr^{+3}, La^{+3}, and Nd^{+3}) this requirement can be satisfied only with bulky multidentate ligands. Other important considerations in precursor design include low decomposition temperatures, decomposition to gaseous by-products, straightforward synthesis and purification, and simple handling.

In the present study the following compounds were found to represent an efficacious embodiment of this strategy: $Ga(dpm)_3$, $Pr(dpm)_3$, $Y(dpm)_3$, $La(dpm)_3$, $Al(acac)_3$, $Sr(hfa)_2$(tetraglyme) and $Ta_2(OCH_2CH_3)_{10}$ (acac = acetylacetonate, dpm = dipivaloylmethanate, hfa = hexafluoroacetylacetonate). The β-diketonate complexes were synthesized from ultrahigh purity metals salts and multiply sublimed prior to use. $Ta_2(OCH_2CH_3)_{10}$ was purchased from Gelest and used under an inert atmosphere without further purification.

Deposition Methodology

In-situ growth of the dielectric thin films was carried out at < 2 Torr in a horizontal reactor with separate, parallel, heated inlet tubes for introducing the precursors into the deposition zone. The precursors were contained in thermostatted Pyrex reservoirs and were introduced immediately up stream of the susceptor. Argon was used as the carrier gas and N_2O (99.0%) was employed as the oxidizing agent. Single crystal $LaAlO_3$ [110] (indexed here in the rhombohedral system[14]) was employed as the substrate. Substrates were heated resistively.

Characterization

The films were initially characterized by SEM for the surface morphology and energy-dispersive x-ray analysis (EDX) for the stoichometry. X-ray diffraction (Ni-filtered, Cu-Kα radiation) was employed for the characterization of crystalline structure, phase purity, and microstructural orientation; θ-2θ scans assessed the crystallinity and phases present, ω-scans (rocking curves) the ç-axis texturing, and ϕ-scans the quality of the in-plane epitaxy. Cross-sectional HREM and TEM were used to further define the microstructure of growth at the film-substrate interface. Film microstructure and chemical environment were further examined by selected area electron diffraction and selected area EDX.

RESULTS

In-Situ Growth of $YAlO_3$ Thin Films

$YAlO_3$ is a promising insulating material for HTS device applications, exhibiting a good lattice match with HTS materials and having excellent dielectric properties ($\varepsilon = 16$; $\tan\delta = 10^{-5}$ at 10 GHz and 77 K).[15] *In-situ* growth of $YAlO_3$ films was achieved using the volatile, precursors $Y(dpm)_3$ and $Al(acac)_3$. The precursors were contained in 100 °C reservoirs and transported to the reaction chamber using Ar carrier gas flowing at 100 and 40 sccm respectively. The N_2O flow rate was 150 sccm. The total system pressure was 1.5 Torr (background pressure = 0.10 Torr) and the film growth temperature was 800 °C.

As evidenced by SEM images, the *in-situ* grown $YAlO_3$ films have smooth mirror-like surfaces. X-ray diffraction θ-2θ scans of the *in-situ* grown $YAlO_3$ films (Figure 1a) reveal phase purity and a high degree of texturing. The coincidence of the (002) and (110) diffraction planes ($2\theta = 24.12^{o}$ for (002), $2\theta = 23.93^{o}$ for (110)) renders initial

differentiation of film growth orientations (001) and (110)) ambiguous (*vide infra*). Diffractometric rocking curves (ω-scan) indicate a high degree of alignment/perfection of the film growth planes with respect to the substrate surface. Thus, the full width at half maximum (FWHM) of the $YAlO_3$ (004)/(220) reflection is 0.44° (Figure 1b) versus 0.11° for the corresponding (220) reflection of the single crystal substrate. A ϕ-scan was also performed to assess the quality of the in-plane epitaxy. In theory, four equivalent planes of reflection should be observed, repeating every 88.37° or 91.63°. A typical ϕ-scan of the <202> family of diffraction planes (Figure 1c) exhibits the requisite two-fold (nearly four-fold) symmetry, hence a high level of in-plane epitaxy.

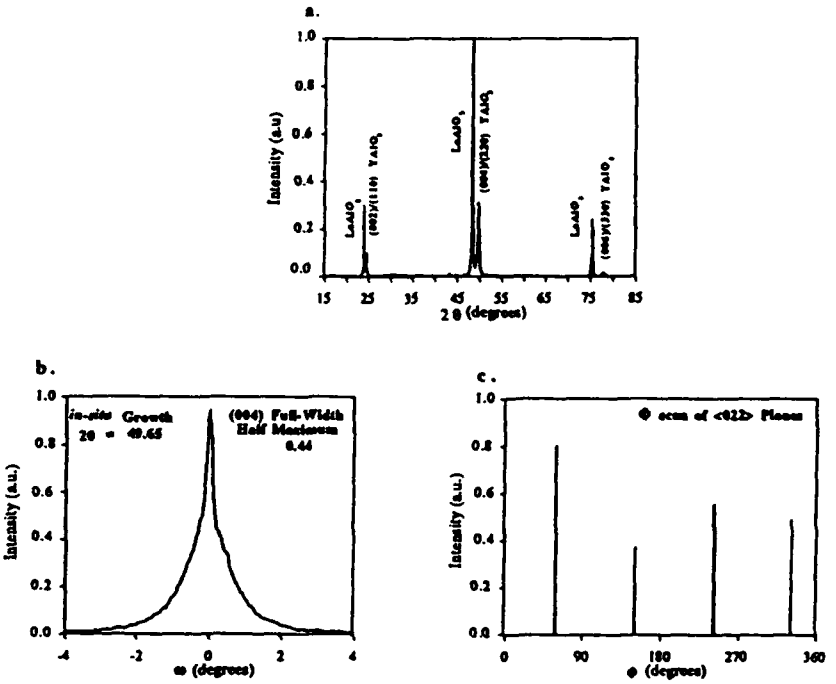

Figure 1. X-ray diffraction of an *in situ* MOCVD-derived $YAlO_3$ film on a $LaAlO_3$ substrate. a. θ-2θ scan, b. ω-scan of YAlO3 (004)/(220) reflection. The FWHM of the reflection is 0.44°, c. ϕ-scan of <022> family of planes.

In-Situ Growth of $PrGaO_3$ Thin Films

$PrGaO_3$ is one of the best YBCO lattice-matched perovskites (misfit ~ 1%), and has good dielectric properties (ε = 24, independent of frequency from 1kHz to 1 MHz and independent of temperature from 16 to 300 °C; tan δ = 3.6 x 10^{-4} - 5.4 x 10^{-3} and varies approximately in proportion to frequency and temperature).[12] *In-situ* growth of $PrGaO_3$ films was carried out using the $Pr(dpm)_3$ and $Ga(dpm)_3$. The precursors were contained in thermostatted (100°C and 130°C respectively) reservoirs and transported to the reaction chamber with Ar flowing at 100 sccm. The N_2O flow rate was 150 sccm. The total system pressure was 1.5 Torr with a background pressure of 0.10 Torr. The growth temperature for the $PrGaO_3$ films was 750-800°C.

As evidenced by SEM images, the *in-situ* grown $PrGaO_3$ films have a smooth mirror-like surface. X-ray diffraction θ-2θ scans of the MOCVD-derived $PrGaO_3$ films reveal that the $PrGaO_3$ films are phase-pure and highly oriented (Figure 2a). The coincidence of the (002) and (110) diffraction planes (2θ = 22.95 for (002), 2θ= 22.93 for (110)) again renders initial differentiation of the (001) and (110) film growth orientations ambiguous (*vide infra*). Diffractometric rocking curves (ω-scans) indicate a high degree of alignment/perfection of the film growth planes with respect to the substrate surface. The $PrGaO_3$ films exhibit a FWHM of the (004)/(220) reflection of 0.47° (Figure 2b) versus

0.11° for the corresponding (220) reflection of the $LaAlO_3$ substrate. In order to assess the quality of the in-plane epitaxy, ϕ-scans were also performed . In theory, four equivalent planes of reflection should be observed, repeating every 89.68° or 91.32°. A typical ϕ-scan of the <202> family of diffraction planes (Figure 2c) exhibits the requisite two-fold (nearly four-fold) symmetry and hence a high level of in-plane epitaxy.

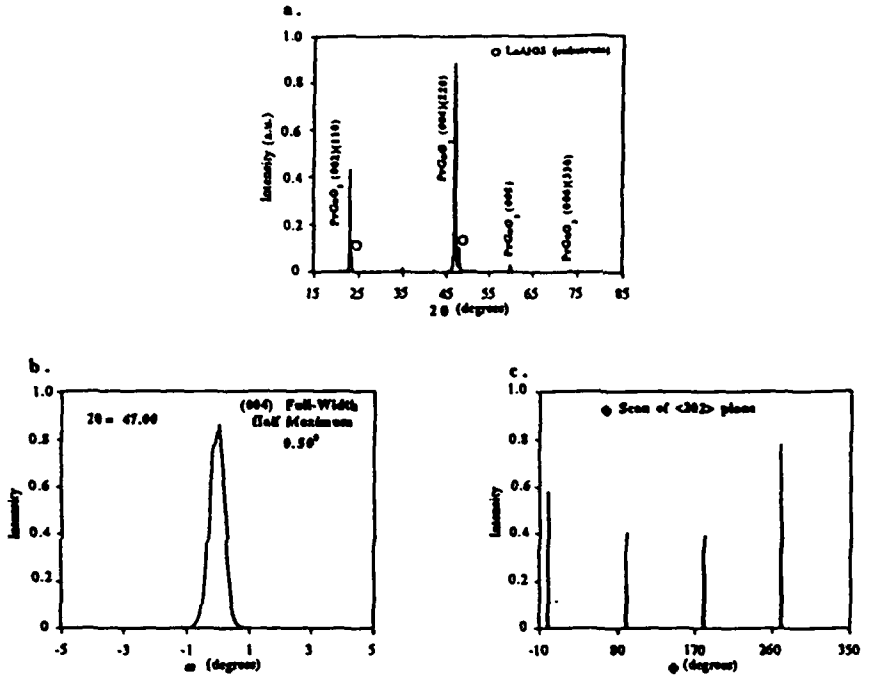

Figure 2. X-ray diffraction of an *in situ* MOCVD-derived $PrGaO_3$ film on a $LaAlO_3$ substrate. a. θ-2θ scan, b. ω-scan of $PrGaO_3$ (004)/(220) reflection. The FWHM of the reflection is 0.50°, c. φ-scan of <022> family of planes.

The suitability of the MOCVD-derived $PrGaO_3$ films as buffer layers for YBCO thin film growth has been demonstrated by pulsed laser deposition (PLD)[16] and pulsed organometallic molecular beam epitaxy (POMBE) techniques.[17] The YBCO films grown by PLD and POMBE on MOCVD-derived $PrGaO_3$ exhibit T_c's of 91 and 89 K, respectively, and J_c's of 6 x 10^6 A/cm^2 at 77 K. These results indicate that MOCVD-derived $PrGaO_3$ performs as a high quality buffer layer.

In Situ Growth of $NdGaO_3$ Thin Films

$NdGaO_3$ is also a YBCO lattice-matched perovskite (misfit ~ 1%) with excellent dielectric properties (ϵ = 22 at 3 GHz and 77 K; tan δ = 3 x 10^{-4} at 5 GHz and 77 K).[25] Growth of $NdGaO_3$ films was carried out *in situ* using the precursors of $Nd(dpm)_3$ and $Ga(dpm)_3$. The sources were set at 100 °C and 140 °C for the Ga precursor and Nd precursor respectively. Deposition of the film was carried out at a system pressure of 1.5 Torr (background pressure = 0.1 Torr) and a substrate temperature of 800 °C. Flow rates of 100 sccm for Ar and 300 sccm for N_2O were routinely used.

X-ray diffraction θ-2θ scans (Figure 3a) reveal that the films are phase-pure and highly textured. The coincidence of (110) and (002) diffraction planes again prevents initial differentiation of (110) and (001) film growth orientation. X-ray diffraction rocking curves were measured for the $NdGaO_3$ films. The FWHM of the (220)/(004) $NdGaO_3$ reflection is 0.48° as determined by a least-squares fitting method (Figure 3b), while the FWHM of the $LaAlO_3$ (220) substrate reflection is 0.11°. X-ray diffraction ϕ scans were performed to determine the quality of the in-plane epitaxy. In theory, four equivalent

planes spaced every 89.29° or 90.71° should be observed. A typical ϕ-scan of the <202> diffraction planes for an MOCVD-derived $NdGaO_3$ film on $LaAlO_3$ shows the requisite, two-fold (nearly four-fold) symmetry, which confirms a high level of in-plane epitaxy (Figure 3c).

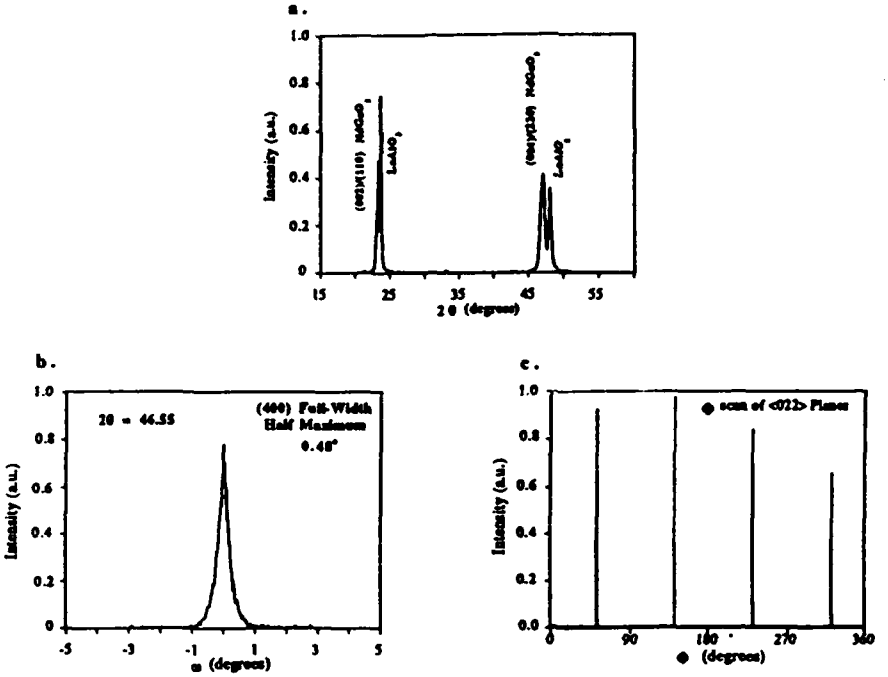

Figure 3. X-ray diffraction of an *in situ* MOCVD-derived $NdGaO_3$ film on a $LaAlO_3$ substrate. a. θ-2θ scan, b. ω-scan of $NdGaO_3$ (004)/(220) reflection. The FWHM of the reflection is 0.48°, c. ϕ-scan of <022> family of planes.

In Situ Growth of Sr_2AlTaO_6 Films

Sr_2AlTaO_6 (SAT) is particularly attractive as an insulating material for use in HTS electronics since it exhibits a good lattice match with YBCO (~ 2%) (Sr_2AlTaO_6 has a cubic structure with $a_o = b_o = c_o = 7.795$ Å;[18] $YAlO_3$, $PrGaO_3$ and $NdGaO_3$ are orthorhombic), a very low reported dielectric constant ($\varepsilon = 11.8$ at room temperature and 100 K) and low dielectric loss ($\tan\delta = 1.68 \times 10^{-3}$ and 4.24×10^{-3} at room temperature and 100 K, respectively).[19] Furthermore, Sr_2AlTaO_6 exhibits no phase transitions between room temperature and 750°C. MOCVD of Sr_2AlTaO_6 films was carried out in a horizontal metal reactor using the metal-organic precursors $Sr(hfa)_2$(tetraglyme), $Al(acac)_3$, and $Ta_2(OCH_2CH_3)_{10}$ as well as the reactant gas N_2O. The precursors were contained in thermostatted flasks at 60 °C, 90 °C, and 130 °C for the Ta, Al, and Sr precursors, respectively, and transported to the reaction chamber by Ar flowing at 60 - 100 sccm. The N_2O was introduced immediately upstream of the susceptor at a flow rate of 150-200 sccm. The total system pressure was 1.5 Torr with a background pressure of 0.10 Torr. The substrates were heated restively at 750-900 °C during film depositions.

X-ray diffraction θ-2θ scans of the MOCVD-derived Sr_2AlTaO_6 films reveal a very large sensitivity of composition and microstructure to the deposition conditions. Films grown at 750 °C are multi-phase and largely unoriented as indicated by θ-2θ scans.[20] Identified phases included Sr_2AlTaO_6, SrF_2, and $SrAl_4O_7$. The source of fluoride is without doubt the hfa ligand. In contrast, films grown at 800 °C with all other conditions identical, yielded phase-pure Sr_2AlTaO_6 films.[20] Diffractometric rocking curves (ω-scans) indicate a low degree of alignment/perfection of the film growth planes with respect to the

substrate surface. The films exhibit a FWHM for the Sr_2AlTaO_6 (400) reflection of 2.03° versus 0.20° for the corresponding (220) reflection of the $LaAlO_3$ single-crystal substrate.[20] In-plane ϕ-scans were also performed to assess the quality of the in-plane epitaxy. In theory, four equivalent planes of reflection should be observed, repeating every 90°. Typical ϕ scans of the <220> family of Sr_2AlTaO_6 diffraction planes grown at 800 °C exhibits the requisite four-fold symmetry, but with rather broad peaks.[20]

Increasing the substrate temperature to 850 °C during deposition results in significant enhancement of growth plane alignment and crystallinity (Figure 4a). Diffractometric rocking curves now exhibit a FWHM for the Sr_2AlTaO_6 (400) reflection of 0.51° (Figure 4b). Typical ϕ scans of the <220> family of Sr_2AlTaO_6 diffraction planes (Figure 4c) exhibit sharp reflections having the requisite four-fold symmetry and hence a high level of in-plane epitaxy.

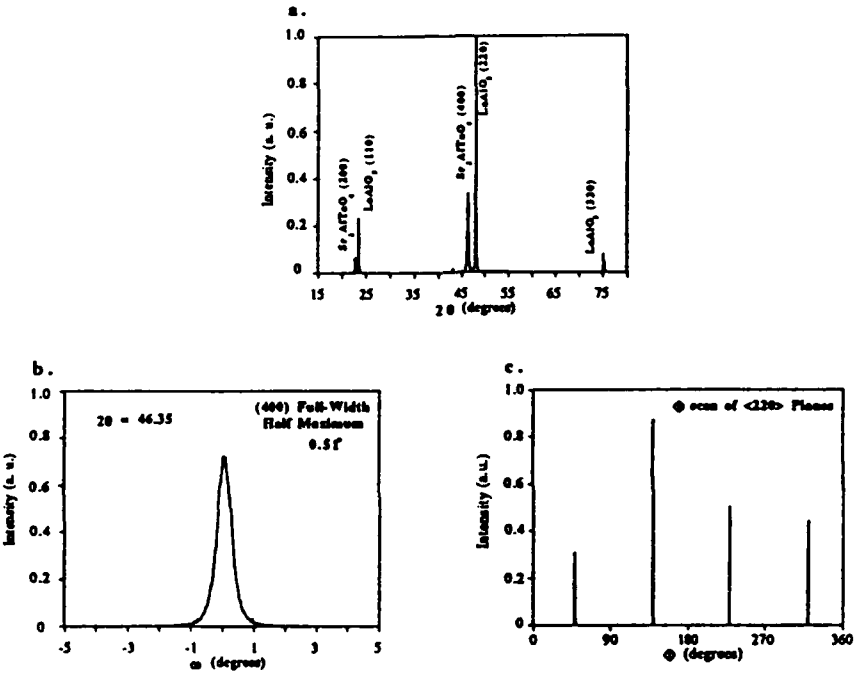

Figure 4. X-ray diffraction of an *in situ* MOCVD-derived Sr_2TaAlO_6 film on a $LaAlO_3$ substrate. a. θ-2θ scan for the film grown at 850 °C. b. ω-scan of (200) reflection of Sr_2TaAlO_6 grown at 850 °C . The FWHM of the reflection is 0.51°. c. ϕ-scan of <022> family of planes for the film grown at 850 °C.

DISCUSSION

One common microstructural feature of the epitaxial $PrGaO_3$, $NdGaO_3$, and $YAlO_3$ films grown on $LaAlO_3$ is epitaxial growth with two growth directions: <001> and <110> and three growth domains as observed by HREM images and TEM selected area diffraction (Figure 5). The same results were also observed by Brorsson et al.[21] when the $PrGaO_3$ was grown on YBCO by laser ablation. The two growth orientation feature is determined by the crystal structure. In the crystal structures of $PrGaO_3$, $NdGaO_3$ and $YAlO_3$ the unit length in the unit cell in the <110> direction is very close to c_0 ($c_0 \approx (a_0^2 + b_0^2)^{1/2}$). Both growth orientations, <001> and <110>, have very close lattice mismatch properties with either YBCO or $LaAlO_3$ on which the dielectric thin films were grown. This indicates that the two growth orientations are both favored for nucleation and growth at ~ 800 °C. Even though films of $YAlO_3$, $PrGaO_3$, and $NdGaO_3$ grow with two directions and three kinds of domains, the microstructures are close to perfectly aligned at the domain boundaries. This

observation means that the three domains exactly match each other at the domain boundaries. With respect to the growth of multilayer structures, a YBCO film can be grown epitaxially on the two coexistent orientations of the buffer films (Figure 5), because both orientations have essentially the same lattice match with YBCO .

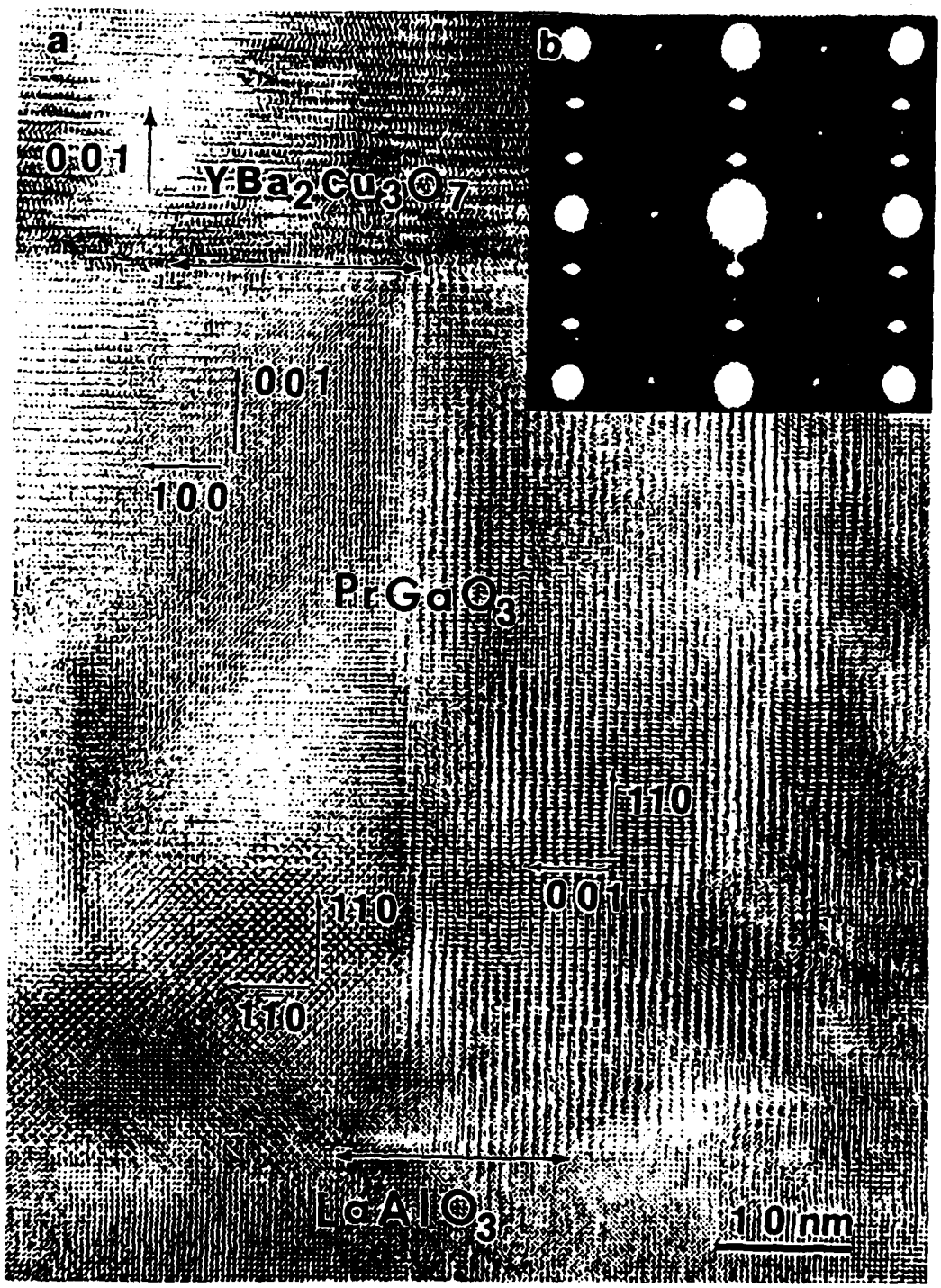

Figure 5. a. Cross-sectional HREM image of a $YBa_2Cu_3O_{7-x}/PrGaO_3/LaAlO_3$ trilayer structure.
b. Selected-area diffraction pattern of a $YBa_2Cu_3O_{7-x}/PrGaO_3/LaAlO_3$ trilayer structure by TEM. The electron beam is perpendicular to the film surface.

CONCLUSIONS

Phase pure thin films of HTS lattice-matched and low dielectric constant and low dielectric loss tangent perovskite insulators $YAlO_3$, $PrGaO_3$, $NdGaO_3$, and Sr_2TaAlO_6 have been grown *in-situ* on single-crystal (110) $LaAlO_3$ substrates by metal-organic chemical vapor deposition (MOCVD). The films exhibit mirror-like smooth surfaces. The films grow epitaxially as shown by X-ray diffraction. As assessed by the HREM images, the films grow with atomically abrupt film-substrate interfaces and the epitaxial growth is further confirmed. The feature of two coexisting growth orientations (<001> and <110>) and three epitaxial growth domains is observed in the MOCVD-derived $PrGaO_3$, $NdGaO_3$, and $YAlO_3$ films. For Sr_2TaAlO_6, a growth temperature of 850°C is required in order to prepare phase pure epitaxial thin films.

ACKNOWLEDGMENT

This research was supported by the National Science Foundation through the Science and Technology Center for Superconductivity (Grant DMR 9120000) and the Northwestern Materials Research center (Grant DMR 9120521) and by DARPA through Contract 91-C-0112. We thank Dr. David A. Rudman, Mr. D. B. Buchholz, and Prof. R.P.H. Chang for growing YBCO films on the MOCVD-derived dielectric buffer films by PLD and POMBE, and Dr. Hong Zhang and Prof. V. P. Dravid for TEM analysis. We thank Drs. G. Wagner and J. Talvacchio for stimulating discusstions.

REFERENCE

1. J. Talvacchio and G.R. Wagner, SPIE Proc. 1292:2 (1990), and references therein.
2. W. Ito, S. Okayama, N. Homma, and T. Morishita, Appl. Phys. Lett. 62:312 (1993).
3. K.H. Young and D.D. Strother, Physica C 208:1 (1993), and references therein.
4. J.M. Philips, M.P. Siegal, R.B. Van Dover, T.H. Marshall, C.D. Brandle, G. Berkstresser, A.J. Strauss, R.E. Fahey, S. Sengupta, A. Cassanho, and H.P. Jenssen, J. Mater. Res. 7:2650 (1992). and references therein.
5. H. Haefke, H.P. Lang, R. Sum, H.J. Guntherodt, L. Berthold, and D. Hesse, Appl. Phys. Lett. 61:2359 (1992).
6. S. Honstu, J. Ishii, and S. Kawai, Appl. Phys. Lett. 59:2886 (1991), and references therein.
7. G. Malandrino, D.S. Richeson, T.J. Marks, D.C. DeGroot, J.L. Schindler, and C.R. Kannewurf, Appl. Phys. Lett. 58:182 (1991), and references therein.
8. J. Zhao, Y.Z. Li, C.S. Chern, P.Lu, B. Norris, B. Gallois, F. Kear, X.D. Casandey, R.E. Wu, Muenchausen, and S.M. Garrison, Appl. Phys. Lett. 59:1254 (1991), and references therein.
9. K. Zhang, and A.Erbil, Materials Science Forum, in press, and references therein.
10. F. Hirai and H. Yamane, J. Crystal Growth 107:683 (1991), and references therein.
11. B. Han, D.A. Neumayer, D.L. Schulz, B J. Hinds, T.J. Marks, H.Zhang, and V.P. Dravid, Chem. Mater. 5:14 (1993).
12. M. Sasaura, M. Mukaida, and S. Miyazawa, Appl. Phys. Lett. 57: 2728 (1990) and references therein.
13. H.J. Scheel, M. Berkowski and B. Chabot, J. Crystal Growth, 115:19 (1991).
14. G.W. Berkstresser, A.J. Valentino, and C.D. Brandle, J. Crystal Growth, 109:467 (1991).
15. H. Asono, S. Kubo, O. Michikawi, M. Satou and T. Konaka, Jpn. J. Appl. Phys. 29: L1452 (1990).
16. B. Han, D.A. Neumayer, T.J. Marks, D.A. Rudman, H. Zhang, and V.P. Dravid, submitted to Appl. Phys. Lett.
17. B. Han, D.A. Neumayer, T.J. Marks, D. B. Buchholz, and R.P.H. Chang, unpublished results.
18. C.D. Brandle and V.J. Fratello, J. Mater. Res. 5:2160 (1990).
19. R. Gou, J. Sheen, A. S. Bhalla, F. Ainger, E.C. Subbarao, L.E. Cross, Defense Advanced Research Projects Agency/Office of Naval Research Workshop on Substrate materials for High T_c Superconductors, Williamsburg, VA, 5-7 February, 1992.
20. B.Han, D.A. Neumayer, B.H. Goodreau, T.J. Marks, H. Zhang, and V.P. Dravid, submitted to Appl. Phys. Lett.
21. G. Brorsson, P. A. Nilsson, E. Olsson, S. Z. Wang, T. Scaeson, and M. Lofgren, Appl. Phys. Lett. 61:486 (1992).

Synthesis and Metal Organic Chemical Vapor Deposition of ^{t}Butyl Substituted Cyclopentadienyls of Barium.

Bruce H. Goodreau, Bruce J. Hinds, and Tobin J. Marks*

Contribution from the Department of Chemistry, the Materials Research Center, and the Science and Technology Center for Superconductivity, Northwestern University, Evanston, Illinois 60208

Metal Organic Chemical Vapor Deposition (MOCVD) of barium containing complex oxide thin films requires the use of compounds with a high and stable vapor pressure. To this end, Ba β-diketonates[1] and more recently β-ketoiminates[2] have been used as volatile molecular precursors for MOCVD of metal oxide thin films. The problem of low volatility source compounds in Ba MOCVD is a result of the small charge to radius ratio of Ba^{+2}. $Ba(dpm)_2$ (dpm = dipivaloylmethane) suffers from compositional variation and oligimerization as a result of the small charge to radius ratio .[3a-c] In the second generation precursor, $Ba(hfa)_2$·tetraglyme (hfa = hexafluoroacetylacetonate), oligimerization is overcome through the use of highly electron withdrawing hfa^- ligands which allow for the coordination of tetraglyme thus saturating the coordination shell of barium resulting in an increase in volatility over $Ba(hfa)_2$.[4a,b] BaF_2 formation has been observed in thin films derived from $Ba(hfa)_2$·tetraglyme and often requires further processing steps to remove the fluoride ions.[4a,5] The development of barium precursor compounds which overcome both the problems of low volatility and BaF_2 formation in thin films is critical to the advancement of MOCVD of barium containing thin films. In order to achieve the desired volatility and vapor pressure stability in a non-fluorinated group 2 metal complex, we have begun investigating encapsulated barium metallocenes[6] as MOCVD precursor compounds. This communication describes the synthesis and characterization of bis(di^{t}butylcyclo-

pentadienyl)barium (**1**) and bis(tri^{t}butylcyclopentadienyl)barium (**2**) and their use as volatile precursors for the growth of $BaPbO_3$ thin films by MOCVD.

The synthesis of di^{t}butylcyclopentadiene and tri^{t}butylcyclopentadiene was carried out using the phase transfer catalyzed method of Vernier and Casserely.[7] The ligands were characterized by their ^1H and ^{13}C NMR spectra. The barium complexes were prepared by stirring barium granules in ammonia gas saturated tetrahydrofuran with the appropriate cyclopentadiene (see reaction 1).[8] Compounds **1** and **2** ($(Cp^{tBu2})_2Ba$ and $(Cp^{tBu3})_2Ba$ respectively) were isolated as base free white solids by sublimation of the crude reaction product after filtration and solvent removal. $(Cp^{tBu2})_2Ba$ and $(Cp^{tBu3})_2Ba$ where characterized by elemental analysis, infrared spectroscopy, ^1H NMR spectroscopy, ^{13}C NMR spectroscopy, and mass spectrometry.[9,10]

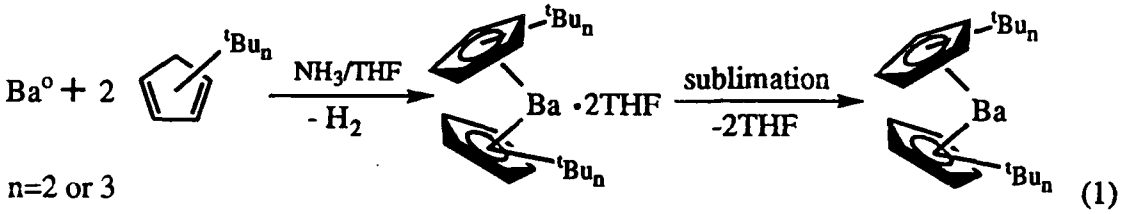

(1)

The chemical and thermal properties of compound **2** suggested that it could be used as MOCVD precursor compounds. Compounds **1** and **2** are both air and moisture sensitive materials. $(Cp^{tBu2})_2Ba$ decomposes immediately upon exposure to the atmosphere, while $(Cp^{tBu3})_2Ba$ only begins to decompose after five minutes. $(Cp^{tBu2})_2Ba$ melted without decomposition from 342°C-346°C while $(Cp^{tBu3})_2Ba$ melted without decomposition from 108°C-110°C. Compounds **1** and **2** sublimed at 210°C and 120°C respectively at $5x10^{-6}$ Torr. The observations above reveal that $(Cp^{tBu3})_2Ba$ has a greater degree of encapsulation of the barium atom than does $(Cp^{tBu2})_2Ba$. The two additional tertiary butyl groups on compound **2** have a marked effect on the physical properties of these compounds. Hanusa has reported similiar changes in melting points and sublimation

temperatures to cyclopentadienyl group 2 metal complexes upon increasing the number of isopropyl groups attached to the cyclopentadienly ring.[6a,b]

The results of the thermogravimetric analysis (TGA) of $(Cp^{tBu3})_2Ba$ is shown in Figure 1 along with those for $Ba(dpm)_2$ and $Ba(hfa)_2$·tetraglyme for comparison.[11] From the thermograms shown on Figure 1, it is evident that $(Cp^{tBu3})_2Ba$ is more volatile than $Ba(dpm)_2$ and only slightly less volatile than $Ba(hfa)_2$·tetraglyme. The TGA trace for $(Cp^{tBu3})_2Ba$ is much narrower than and shows much less residue than the TGA trace for $Ba(dpm)_2$. In terms of volatility and vapor pressure stability, $(Cp^{tBu3})_2Ba$ is superior to $Ba(dpm)_2$. In comparison to $Ba(hfa)_2$·tetraglyme, $(Cp^{tBu3})_2Ba$ has a similar sublimation onset temperature, but has a broader weight loss curve. While the volatility is slightly below $Ba(hfa)_2$·tetraglyme, $(Cp^{tBu3})_2Ba$ contains no fluorine thus alleviating the possibility of BaF_2 formation in thin films. All of these observations taken together suggested that $(Cp^{tBu3})_2Ba$ could be useful as a fluorine free barium MOCVD source compound.

MOCVD experiments were carried out in a hot walled low pressure quartz tube MOCVD reactor and the resulting thin films were characterized by scanning electron miscroscopy (SEM), elemental determination by x-ray analysis (EDX), x-ray photoelectron spectroscopy (XPS), and x-ray diffraction (XRD). The $(Cp^{tBu3})_2Ba$ was placed in an open ceramic crucible in the sublimation zone and heated externally. The substrate, yttria stabilized zirconia or magnesium oxide, was mounted on a quartz holder in the deposition zone which was also heated externally. The temperature of the substrate was monitored by a thermocouple fed through to the back side of the substrate holder. The background pressure of the system was 10^{-3} Torr. No carrier gas was used. Addition of an oxidizer gas such as O_2 caused the $(Cp^{tBu3})_2Ba$ to decompose on the walls of the reactor in the sublimation zone and in the crucible. In a typical experiment, the substrate was heated to 615°C and the sublimation zone was then heated to 110°C. The $(Cp^{tBu3})_2Ba$ melted and then was transported cleanly to the deposition zone. A small amount of $(Cp^{tBu3})_2Ba$

sublimed through the deposition zone and condensed on the walls of the reactor just downstream of the deposition zone. After two hours a shiny grey metallic-like film coated the walls of the reactor and the substrate. Analysis of the films by SEM/EDX and XPS showed that they contained Ba and C, but the film was found to be amorphous by X-ray diffraction. The Ba/C films were insoluble in acetone, water, HCl, and aqua regia. Annealing the Ba/C film in PbO/O_2 at 900°C and one atmosphere for two hours yielded polycrystalline $BaPbO_3$ as shown by x-ray diffraction (Figure 2). A small amount of Ba^0 remained in the $BaPbO_3$ films even after repeated PbO/O_2 annealing . The observation of Ba^0 was quite remarkable considering the highly oxidizing conditions of the anneal. The Ba^0 might result from the formation of a $BaPbO_3$ layer protecting small crystallites of Ba^0. Analysis of the $BaPbO_3$ film by XPS showed that in addition to Ba, Pb and, O the film contained some carbon. The SEM image of the amorphous Ba/C film revealed that the surface was very smooth while the surface the $BaPbO_3$ was quite rough (Figure 3). Post annealing procedures typically have this effect on film morphology.[12]

We have demonstrated the ease in which compounds **1** and **2** can be synthesized by the ammonia gas saturated tetrahydrofuran method. This method offers a very simple alternative to the metathesis of BaI_2 with $K(Cp^{tBun})$ which requires the preparation and purification of $K(Cp^{tBun})$. $(Cp^{tBu3})_2Ba$ is a highly volatile and fluorine free MOCVD precursor as evidenced by its use in the fabrication of $BaPbO_3$ films. The essential component which makes $(Cp^{tBu3})_2Ba$ a useful MOCVD precursor is the tri-^{t}butylcyclopentadiene ligand. Tri^{t}butylcyclopentadiene affords highly volatile thermally stable barium compounds which are easily decomposed under MOCVD conditions. Further work is in progress to address the question of oxygen stability under the conditions necessary for the *in situ* deposition of metal oxides.

Acknowledgments. This work was supported by DARPA (contract # 91-C-0112) administered by Westinghouse Electric Corp. We thank Northwestern University Materials Research Center for access to x-ray diffraction facilities.

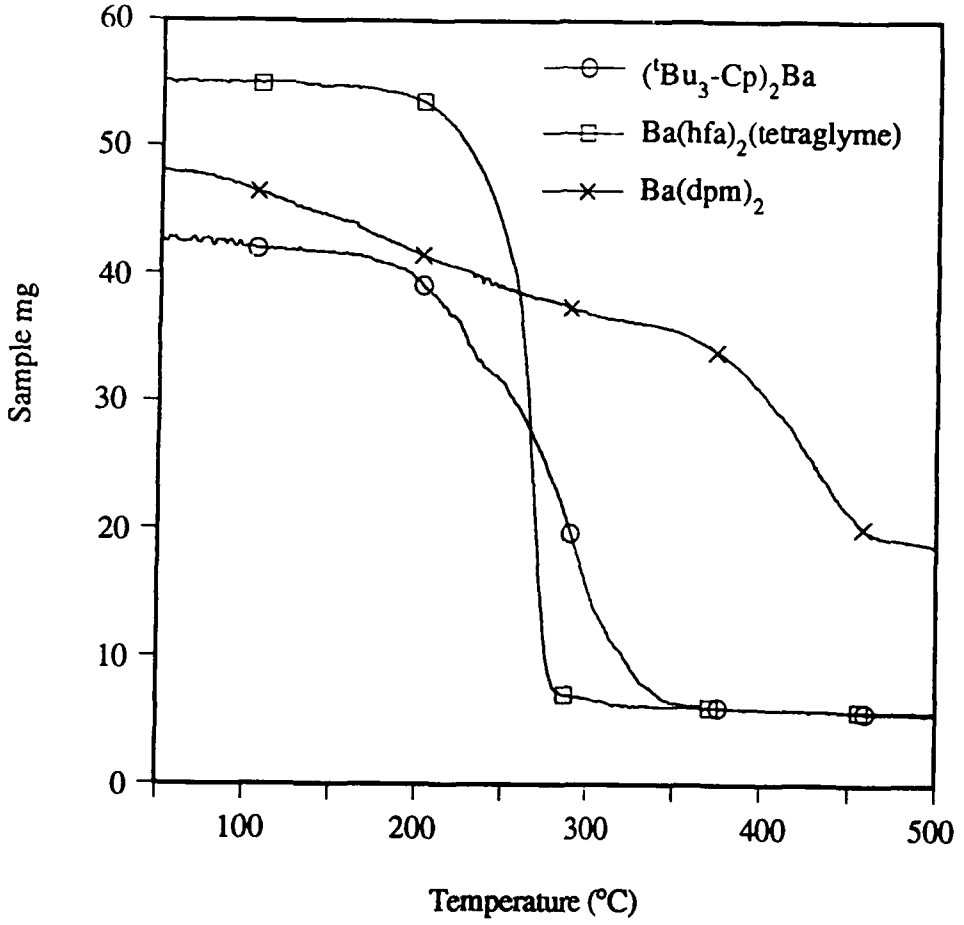

Figure 1. Thermograms of $(Cp^{tBu3})_2Ba$, $Ba(dpm)_2$, and $Ba(hfa)_2$·tetraglyme.

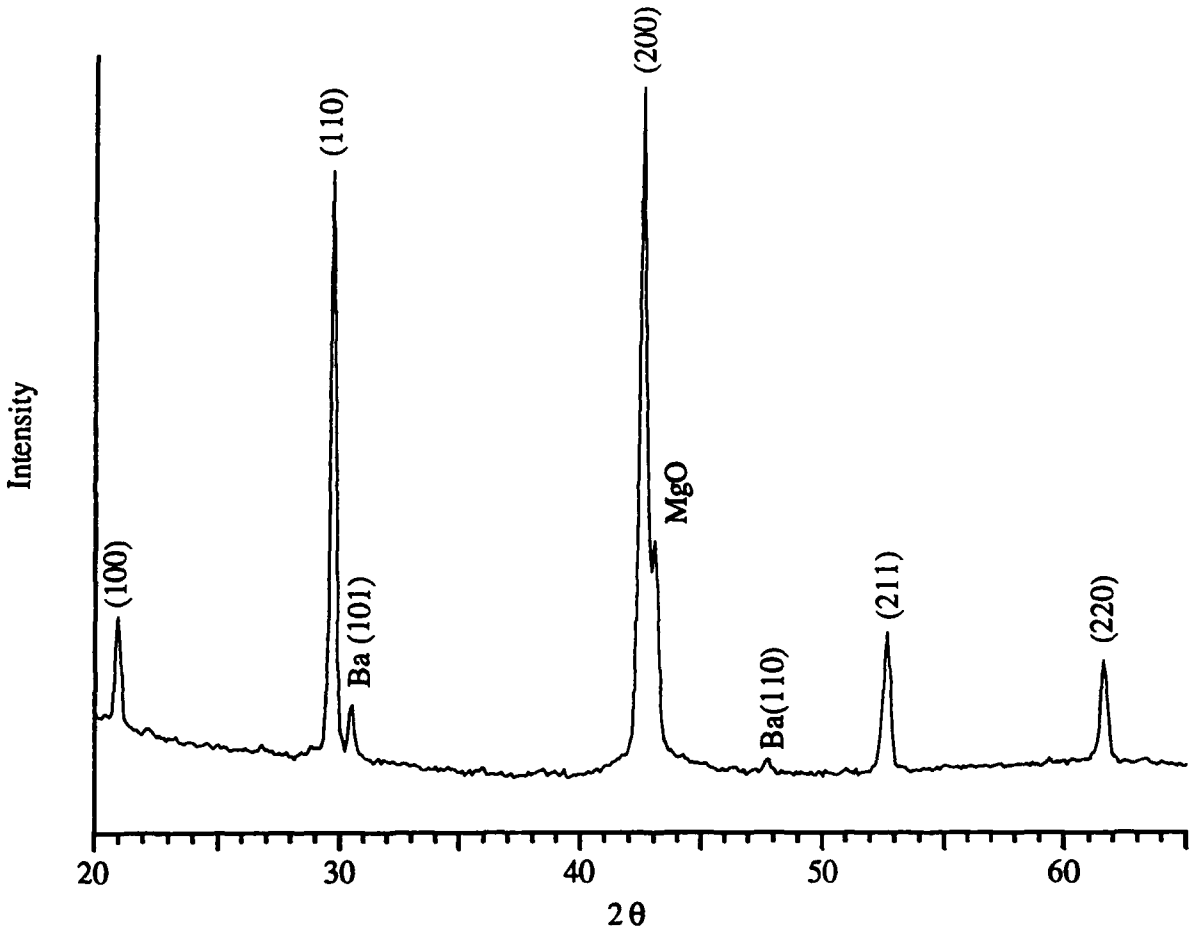

Figure 2. X-ray diffraction pattern of an MOCVD derived $BaPbO_3$ film on MgO.

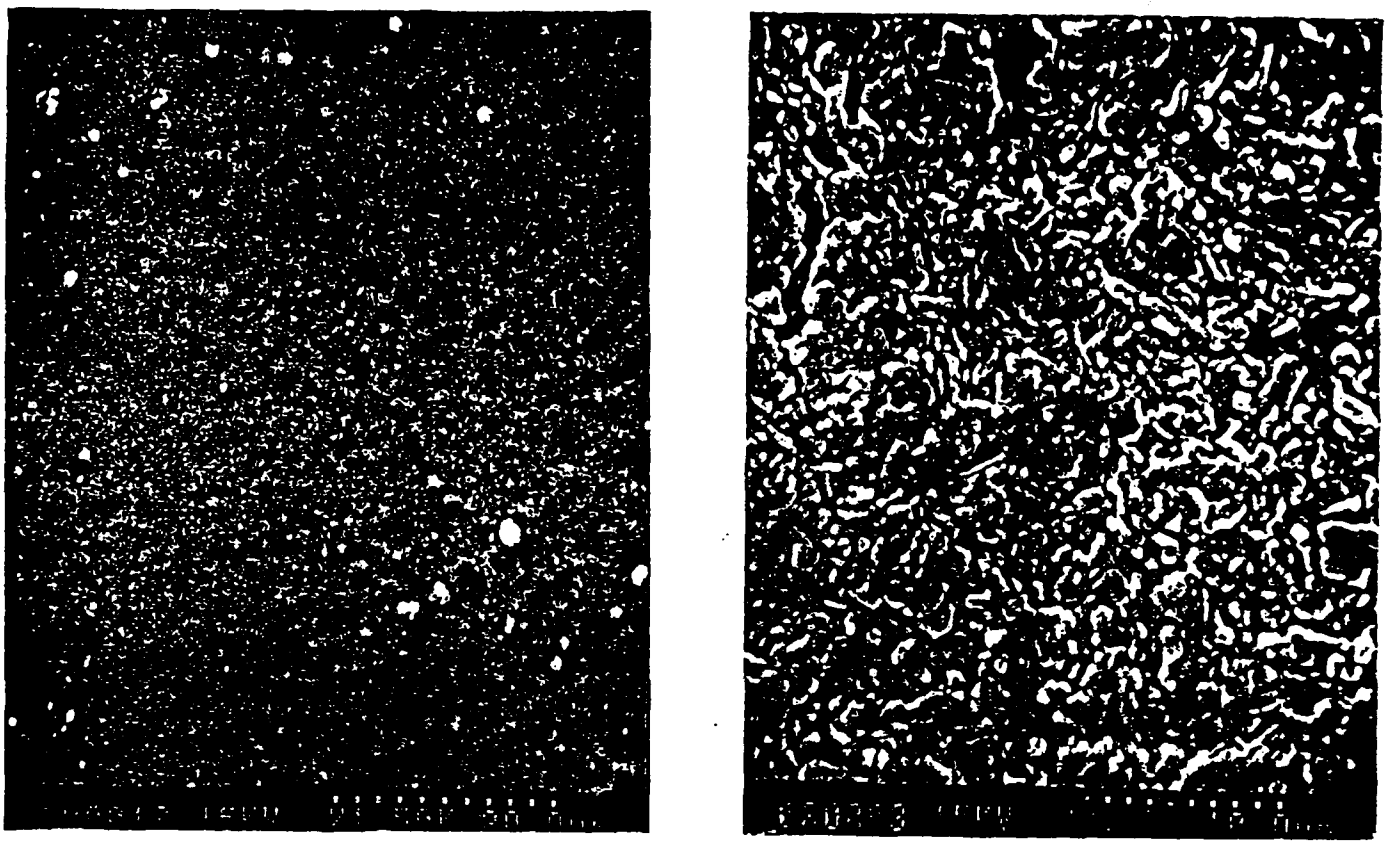

(a) (b)

Figure 3. SEM images of thin films derived from the MOCVD of $(Cp^tBu_3)_2Ba$ (a) amorphous Ba/C film (b) $BaPbO_3$ film.

References

1. Tong, L.M.; Richeson, D.S.; Marks, T.J.; Zhao, J.; Zhang, j.; Wessels, B.W.; Marcy, H.O.; Kannewurf, C.R. Advances in Chemistry Series **1990** *226*, 351 and references therein.

2. Schulz, D.L.; Hinds, B.J.; Stern, C.L.; Marks, T.J. *Inorg. Chem.* **1993**, *32*, 249.

3. (a) Turnipseed, S.B.; Barkley, R.M.; Sievers, R.E.; *Inorg. Chem.* **1991**, *30*, 1164. (b) Gleizes, A.; Sans-Lanain, S.; Medus, P.; Morancho, R.; *C.R. Acad. Sci. Ser. 2* , **1991** *312*, 983. (c) Rossetto, G.; Polo, A.; Benetollo, F.; Porcia, M.; Zanella, P. *Polyhedron*, **1992**, *11*, 979.

4. (a) Timmer, K.; Spee, C.I.M.A.; Mackor, A.; Meinema, H.A.; Spek, A.L.; Vandersluis, P. *Inorg. Chima. Acta.* **1991**, *190*, 109. (b) Schultz, D.L.; Neumeyer, D.; Marks, T.J. *Inorg. Synth.* submitted.

5. (a) Malandrino, G.; Richeson, D.S.; Marks, T.J.; DeGroot, D.C.; Schindler, J.L.; Kannewurf, C.R. *Appl. Phys. Lett.* **1991**, *58*, 182. (b) Zhang, J.M.; Wessels, B.W.; Richeson, D.S.; Marks, T.J.; DeGroot, D.C.; Kannewurf, C.R. *J. Appl. Phys.* **1991**, *69*, 2743. (c) Duray, S.J.; Buchholtz, D.B.; Song.S.N.; Richeson, D.S.; Ketterson, J.B.; Marks, T.J.; Chang, R.P.H. *Appl. Phys. Lett.* **1991** *59* 1503.

6. (a) Burkey, D.J.; Williams, R.A.; Hanusa, T.P. *Organometallics* **1993**, *12* , 1331. (b) Williams, R.A.; Tesh, K.F.; Hanusa, T.P. *J. Am. Chem. Soc.* **1991**, *113*, 4843.

7. Vernier, C. G.; Casserly, E.W. *J. Am. Chem. Soc.* **1990**, *112*, 2808.

8. Drake, S.R.; Otway, D.J.; *J. Chem. Soc. Chem. Comm.* **1991**, 517.

9. 69.5% yield. mp. 342°C-347°C. Anal. for $C_{26}H_{42}Ba$; Calc'd: 63.43% C, 8.60% H, Found: 63.30% C, 8.67% H. ^1H NMR (toluene d-8): δ 1.28 (s, 36H), 5.60 (br t, 2H, J~2Hz), 5.93 (d, 4H, J=2.4Hz). ^{13}C NMR (toluene d-8): δ 32.30 $\underline{C}(CH_3)_3$, 33.03 $C(\underline{C}H_3)_3$, 103.25 ring $\underline{C}H$, 105.61 ring $\underline{C}H$, 136.48 $\underline{C}$-^{t}Bu. IR (Nujol mull): 3058 (w), 3063)w, 1364 (s), 1353 (s), 1250(s), 1199 (m), 1162 (m), 1050 (w), 1043 (w), 1017 (w), 933 (w), 802 (s), 782 (s), 730(s), 687 (m), 673 (m), 663(m). Mass Spec. (EI, 70 eV): 492 (M^+ envelope, mass: obs.(calc) 489: 9.0(9.7), 490: 13.5(13.1), 491: 13.5(13.1), 492: 100(100), 493: 27.9(28.4), 494: 2.1(4.0)), 410 (M^+ - HCC-^{t}Bu), 315 (M^+ - Cp^{tBu}_2).

10. 10.6% yield. mp. 108°C-110°C. Anal. for $C_{34}H_{58}Ba$; Calc'd: 67.59% C, 9.68% H, Found: 67.68% C, 9.66% H. ^1H NMR (toluene d-8): δ 1.28 (s, 18H), 1.38 (s, 36H), 5.78 (s, 4H). ^{13}C NMR (toluene d-8): δ 32.11 $\underline{C}(CH_3)_3$, 33.03 $C(\underline{C}H_3)_3$, 33.60 $\underline{C}(CH_3)_3$, 34.66 $C(\underline{C}H_3)_3$, 108.42 ring $\underline{C}H$, 130.36 ring $\underline{C}$-^{t}Bu, 132.53 ring $\underline{C}$-^{t}Bu. IR (Nujol mull): 3093 (w), 3078(w), 1385 (m), 1363 (m), 1355 (s), 1237 (s), 1195 (w), 1160 (w) 1002 (w), 790 (s), 675 (w). Mass Spec. (EI, 70 eV): 604 (M^+ envelope, mass:obs(calc.), 601:8.7(9.8), 602:13.2(13.7), 603:17.6(19.2), 604:100(100), 605:34.8(36.8), 606:5.3(6.7)), 371 (M^+ - Cp^{tBu}_3)

11. Han, B.; Neumayer, D.; Schulz, D.L.; Marks, T.J.; Zhang, H.; Dravid, V.P. *Appl. Phys. Lett.*, in press.